Low Frequency Interference on the VLA and its Removal

W. D. Cotton, November 2009, (rev. February 4, 2010)

***Abstract*—This memo explores the proprieties of the interference in 74 MHz data from the VLA and techniques for removing its effects. An RFI excision technique to estimate and subtract the contributions of quasi–continuous interfering signals based on the difference in phase rotation of terrestrial and celestial signals is explored. A specific implementation is developed and applied to a number of instances of VLA 74 MHz data sets and shows a significant potential for reducing the effects of interference when combined with traditional flagging of impulsive interference. While the technique has only been applied to VLA 74 MHz data it should be applicable to other cases of quasi-continuous interference.**

***Index Terms*—interferometry, interference**

I. Introduction

THE weak signals from the celestial sources observed by radio interferometers are easily swamped by signals of a closer origin; even inside of the protected radio astronomy bands. Mitigating the effects of these interfering signals is a major concern in the construction and operation of radio telescopes. This interference is referred to as "Radio Frequency Interference" or RFI but the actual interfering signal need not have been emitted at the sky frequency of the telescope.

Most of the off-line data processing techniques for dealing with RFI in the past have consisted of identifying such signals and "flagging" the data – effectively deleting the data affected. These techniques only really work for interference that is impulsive in time and/or frequency and can be detected by contrast with unaffected data. Quasi–continuous and especially broadband signals are not readily susceptible to this treatment as all data may be affected.

Recent work [1] has explored alternate approaches, separating the celestial and terrestrial signals and subtracting the interfering signals from the data. In the following, estimation and subtraction of interfering signals will be referred to as "excision".

This memo investigates the nature of the interfering signals seen in VLA 74 MHz data and explores techniques, both flagging and excision, for reducing their effects on derived images. The techniques described here have been implemented in the imaging software in the Obit package [2] [1].

II. Properties of VLA 74 MHz Interference

The interfering signals in VLA 74 MHz data come in a variety of forms, narrow band, wide-band, impulsive and continuously varying; all are believed to be generated by the instrument itself. The effects of these signals are best seen in a graphical tool such as AIPS [2] task SPFLG; dynamic spectra of interfering signals are shown in the left hand plots in Figures 1 and 2.

A visual examination of 74 MHz data sets show that many baselines exhibit a comb of narrow band signals, of which Figure 2 shows an extreme example. On a number of baselines, broadband signals are also seen as in Figure 1. The relative rarity of these broadband signals and the lack of correlation with baseline length or proximity to the control building suggest that these signals are not entering the system through the telescope feeds but may be entirely internal to the instrument. Irrespective of the origin of these signals, most are at least quasi–continuous in nature and thus subject to excision techniques.

III. RFI Excision

A. Athreya's Technique

The RFI excision technique of Athreya[1] developed for GMRT observations is to use the fact that terrestrial signals will have a constant phase with respect to the interferometer whereas the rotation of the earth causes celestial sources to have a time variable phase. Interferometers track the phase and group delay of celestial sources to remove the effects of earth rotation; this causes any stationary interfering signal to rotate in phase and delay and a source at the phase tracking center to have constant phase. Athreya's technique is to fit for a constant celestial complex signal and an RFI signal whose phase rotates at the opposite rate of the interferometer fringe tracking. The estimate of the RFI can then be subtracted from the data leaving, in principle, only the response to the celestial sources. This process is performed on each baseline, frequency channel and polarization independently. For this technique to work, the data must be well sampled in each turn of the fringe tracking phase.

One of the difficulties with this approach is that the amplitude of the interfering signal may be time varying, due to motion of the signal through the side–lobes or other changing circumstances. Thus, there is an upper limit to the amount of time that can be used to separate the celestial and interfering signals. When the interferometer fringe rates become sufficiently low, it is no longer possible to use this approach to separate the signals. A further complication is that sources far from the phase tracking center will have a

National Radio Astronomy Observatory, 520 Edgemont Rd., Charlottesville, VA, 22903 USA email: bcotton@nrao.edu

[1] http://www.cv.nrao.edu/∼bcotton/Obit.html

[2] http://www.aips.nrao.edu/

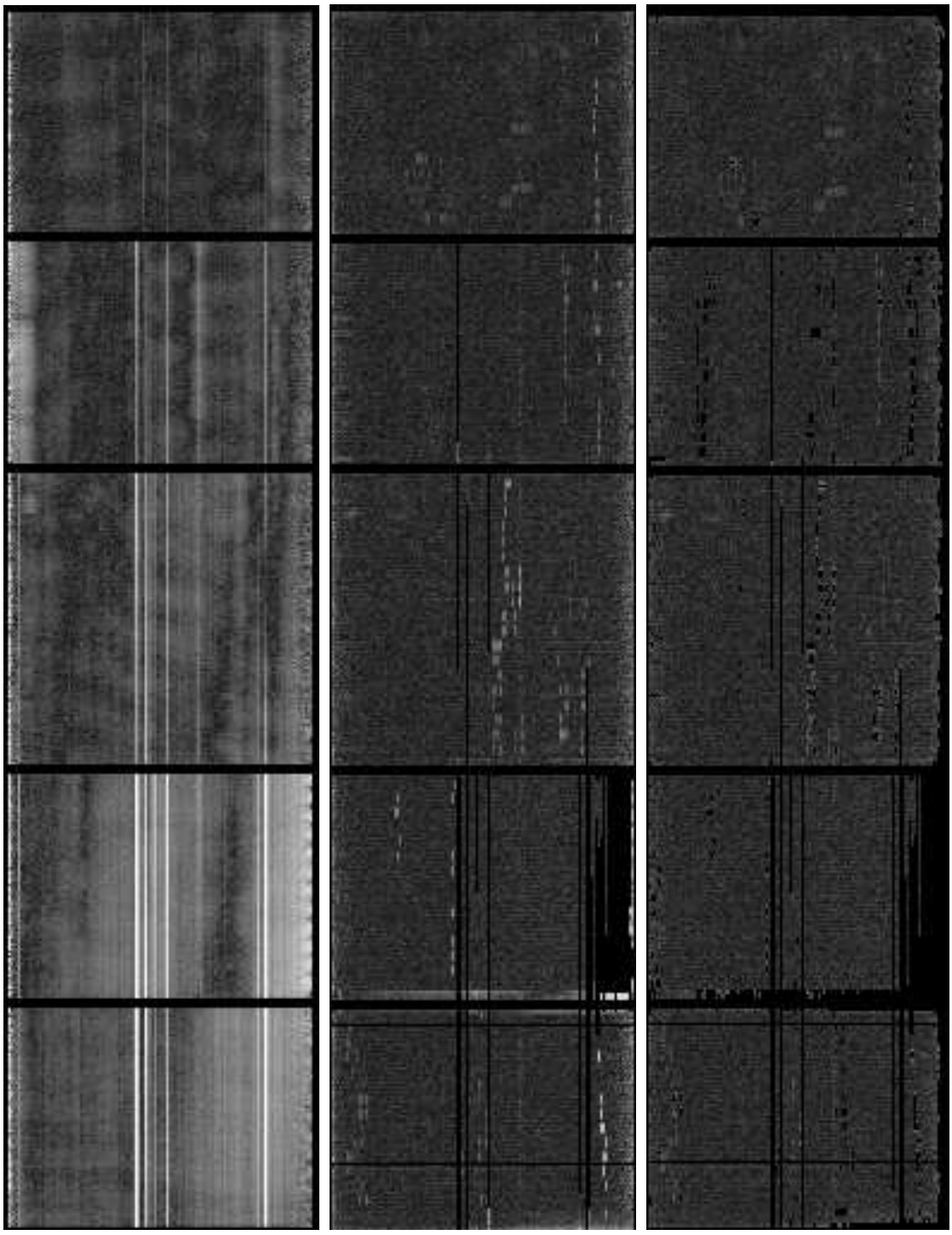

Fig. 1. Dynamic spectra of baseline 8–22 RR data from Example 1 in various stages of processing, all with the same stretch. Time flows from the bottom upwards and the 127 frequency channels are shown on the horizontal axis. Left is the residual data with no interference removed; Center is after initial clipping and RFI excision; Right is after RFI excision and clipping excessive amplitude data. Data consists of 5 $\times$ 15 minute scans spread over several hours. The amplitudes saturate at 10,000 Jy.

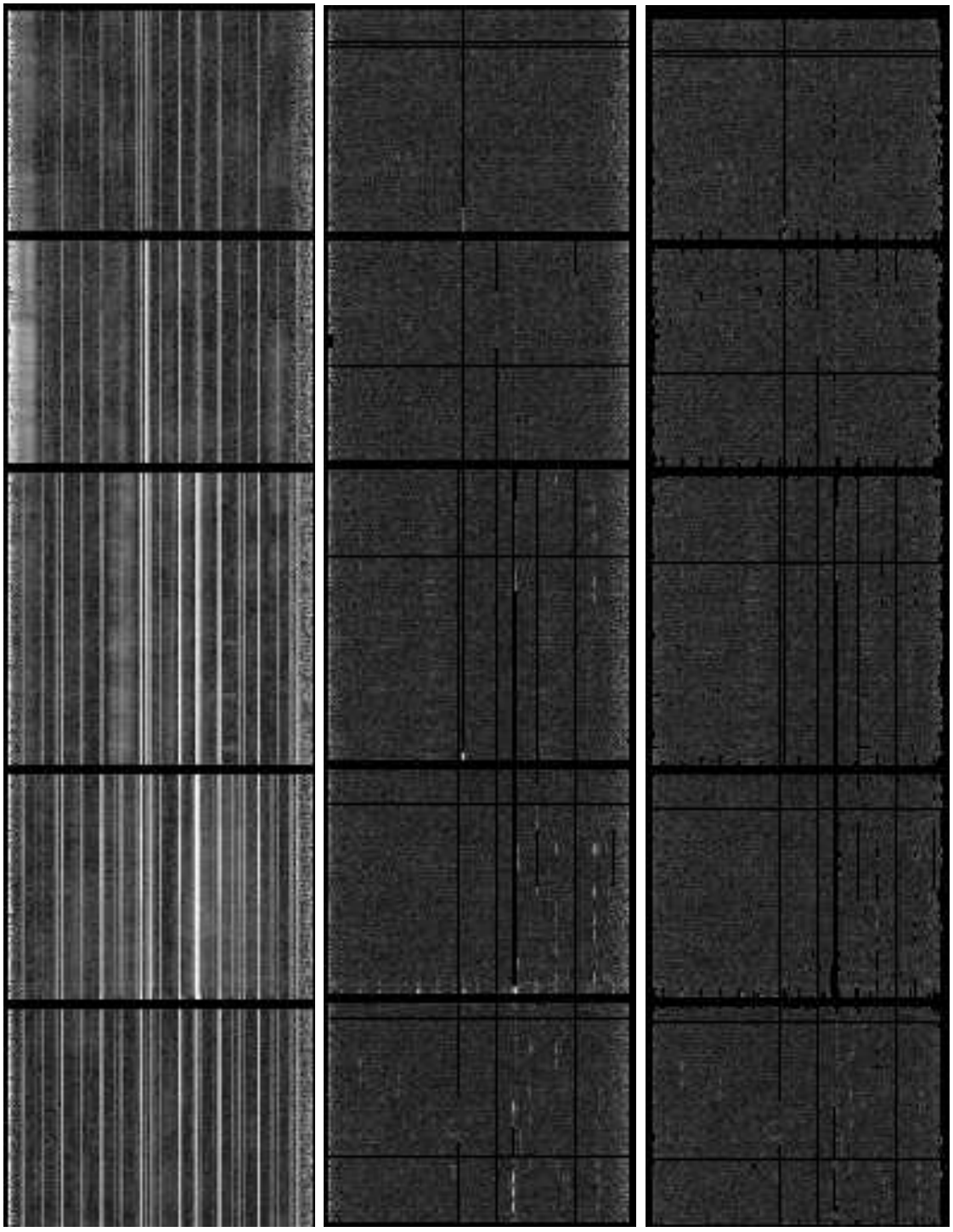

Fig. 2. Like Figure 1 but for baseline 2–11, LL.

non–zero fringe rate and may have variable phase during the fitting interval.

B. Residual Based Technique

In many cases, it is possible to image a data set in spite of interference. The derived image may be degraded by the interference but at least provides an initial estimate of the sky brightness distribution. The interferometer response to the sky model can be calculated and subtracted from a dataset and these residuals used to estimate the interfering signal.

Instead of using least squares fitting to separate the remaining celestial signal from the interfering signal, it is possible to counter rotate the residual data by the (reverse of) the fringe tracking used in the observation. This will cause a constant terrestrial signal to be constant in time but any residual celestial response to rotate in phase. Subsequent time averaging will tend to wash out the rotating celestial signal but not affect the, now constant, interfering signal. The time averaged, counter rotated residual data can then be used as an estimate of the interfering signal, this is referred to in the following as the "RFI model".

Interfering signals are not expected at all times and frequencies/polarizations (although these conditions may exist) so it is important to select which portions of the averaged, counter–rotated residual data represent RFI and which don't. The simplest criterion is the amplitude of the RFI estimates; true RFI should be well above the level of fluctuations due to the thermal noise in the data; RFI model data with amplitudes below some threshold can be set to zero.

Further criteria are based on the fringe rate. If there are sufficient turns of phase in the fundamental data integration time, then any RFI will largely have canceled out leaving only the signals being tracked by the interferometer. In this case, the averaged, counter–rotated residual data is unlikely to represent interference and the RFI model can be set to zero. The low fringe rate case is still a problem as there will be little reduction of any residual celestial signal by the averaging. If there is possibly significant residual celestial signal, this data should be flagged as its use will subtract sky structure as well as RFI. However, if the sky model subtracted is sufficiently accurate, the RFI model data may be used.

IV. Obit Implementation

The fundamental implementation of the residual based technique is in the c library with interfaces from python and a compiled task.

A. Counter–rotation

Counter–rotation of the interferometer model is performed by calculating the inverse of the interferometer fringe tracking model and creating a Solution (AIPS SN) table with the required values. Application of this calibration table will do the required counter–rotation. The calculation is performed in ObitTableSNUtil.c utility routine ObitTableSNGetZeroFR. A python user interface to this routine is UV.PTableSNGetZeroFR in ObitTalk.

This model calculation uses the baseline UVW vector calculated from the baseline vector b (VLA coordinate system), hour angle ha and source declination δ

$$uvw[0] = b[0] * sin(ha) + b[1] * cos(ha)$$

$$uvw[1] = -vw * sin(\delta) + b[2] * cos(\delta)$$

$$uvw[2] = vw * cos(\delta) + b[2] * sin(\delta)$$

where $vw = b[0] * cos(ha) - b[1] * sin(ha)$.

The fringe rate is then [3]:

$$rate \ = \ uvw[0] * cos(\delta) * \Omega_E/\nu$$

where Ω_E is the Earth's rotation rate and ν is the interferometer sky frequency. The group and phase delays are:

$$\tau \ = \ -uvw[2]/\nu$$

.

B. Residual Based RFI Subtraction

The RFI estimation and subtraction based on residual visibility data is implemented in the Obit class ObitUVRFIXize with a python interface in class UVRFIXize. This operation is also implemented as task LowFRFI. The following parameters control the operation of task LowFRFI.

- **timeAvg**
  Time interval over which to average residual data to estimate RFI (min). This should be as long as the RFI can reasonably be considered constant. NB: if this is too short (less than a half dozen integrations) LowFRFI will artificially reduce the noise as well as remove source emission left in the residual data.
- **minRFI**
  Minimum RFI amplitude (Jy) to remove. This should be set relatively conservatively, at least several sigma in the averaged residual data to keep from merely subtracting noise and any unmodeled flux density.
- **timeInt**
  The averaging time of the input and residual data.
- **solInt**
  The time interval for calculating the counter–rotation SN table
- **doInvert**
  If True, then invert the phase solutions for the counter-rotation SN table. This MAY be needed for GMRT data; do not use for VLA data.
- **minRot**
  The minimum fraction of a turn of phase of the fringe tracking below which to flag output data for which the RFI model exceeds minRFI. This may result in a substantial amount of data being flagged. A low (0) value may be used if a very good model has been subtracted from the data; otherwise extended emission may be removed with the RFI.
- **maxRot**
  The maximum fraction of a turn of phase of the fringe tracking above which the RFI is assumed to have been

washed out. Data for which the phase turns by more than this amount will have no RFI correction made.

The basic RFI excision operation consists of three steps:

1) **Counter–rotation**
   The residual data is counter–rotated by the inverse of the interferometer model and then time averaged to a specified interval (timeAvg). This produces the RFI model. This operation is done in routine ObitUVRFIXizeCounterRot.
2) **Filtering**
   The RFI model is filtered by one of three operations; Nothing - allowing them to be subtracted from the observed visibilities, zeroed - resulting in no modification of the observed visibilities, or flagged - causing corresponding visibilities to be flagged.
   The RFI model is flagged for values whose amplitudes are above minRFI when the total phase rotation during timeAvg is less than minRot. The RFI model is zeroed where the amplitudes are below minRFI or when the total phase rotation during timeInt exceeds maxRot. This operation is done in routine ObitUVRFIXizeFilter.
3) **Correction**
   The filtered RFI model is interpolated to the time of each observed visibility and either is subtracted from the observed visibility or causes it to be flagged. This operation is done in routine ObitUVRFIXizeCorrect.

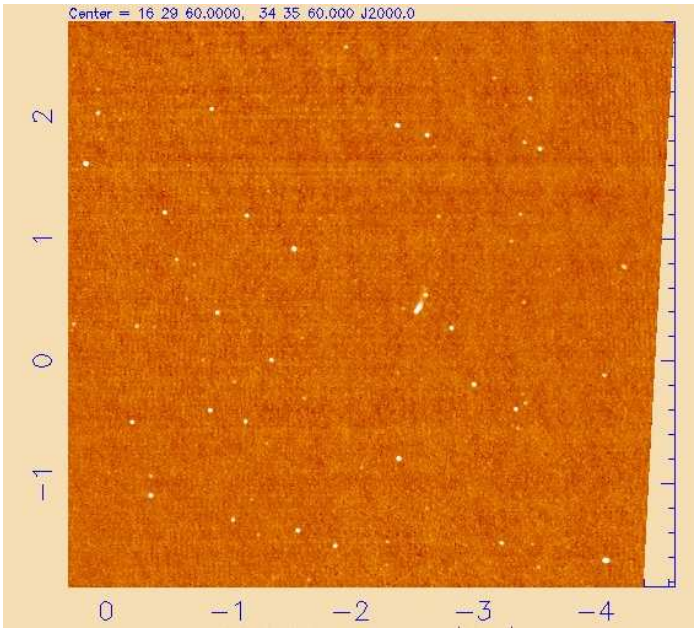

Fig. 6. Image of section of the Example 2 field without removing interference. The interferences is visible in the horizontal banding. The scale in degrees is shown on the side of the image. The RMS in the center portion of the image is 78.4 mJy. Image is the square root of a selected range of pixel values.

V. Examples from VLSS data

In the following the technique described above will be applied to VLA data from the VLSS survey [4]. This data was obtained at 74 MHz using a bandwidth of 1.5 MHz and used 127 channels in RR and LL correlations from the VLA in B configuration. Each pointing was observed for 75 minutes in multiple scans spread over several hours. These data were all obtained under relatively benign ionospheric condition.

A. Example 1: Single baseline tests

1) Single channel: Figure 3 shows data from one scan/baseline/channel/polarization after subtraction of a sky model derived in an initial imaging using Obit task IonImage [5]. Figure 4 shows the RFI model derived from this data with one minute averaging and Figure 5 shows the residuals after subtracting the RFI model. The residuals after subtracting the RFI model are mostly below 100 Jy but in periods of rapid variation of the interference, exceed 200 Jy. The interfering signal is reduced by an order of magnitude.

2) Multiple channels: The middle plots of Figures 1 and 2 show the residuals after subtracting the RFI model from the initial residual data for all channels from one baseline and polarization. Prior to determining the RFI model, residuals values in excess of 10,000 Jy were flagged. The RFI model subtracted data shown in the middle plots still contain occasional large values, a subsequent clipping of values above 500 Jy results in the right–most plots in Figures 1 and 2 which are relatively clean.

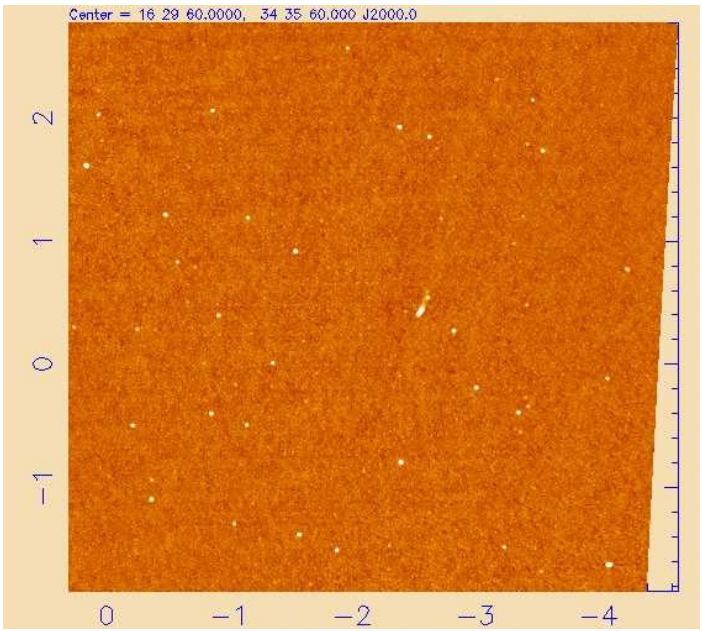

Fig. 7. Like Figure 6 but only removing interference from the high frequency resolution data; some residual interference is still visible. The RMS in the center portion of the image is 76.4 mJy. Image is the square root of a selected range of pixel values.

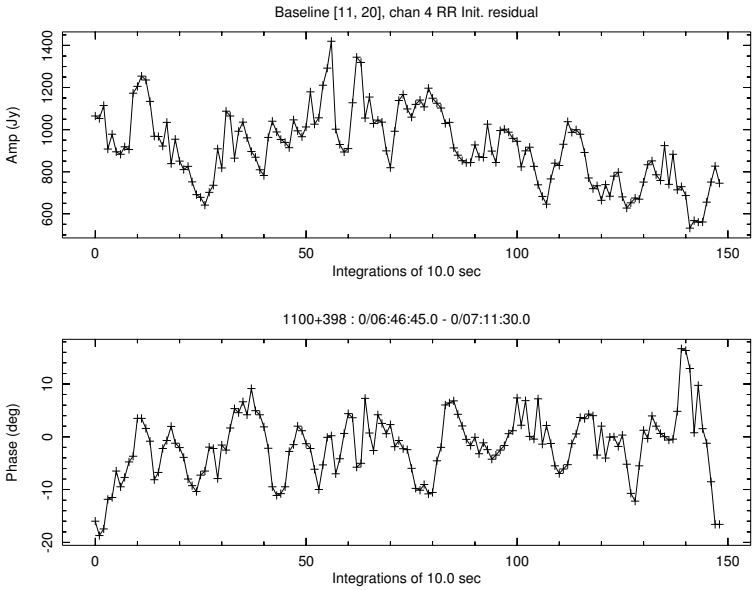

Fig. 3. Residual data for one scan/baseline/channel/polarization. Amplitude is shown on the top, phase on the bottom.

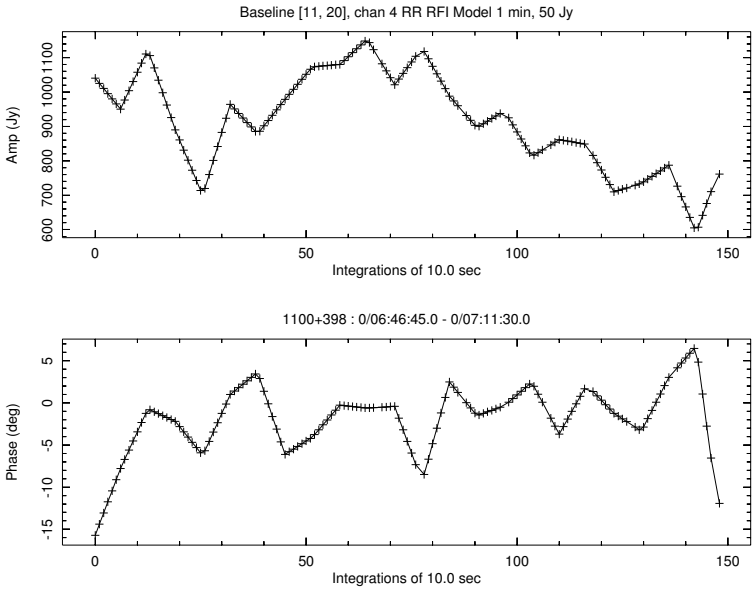

Fig. 4. RFI model for data shown in Figure 3

B. Example 2: High Resolution RFI Excision/Flagging

Once the RFI model is derived from an initial imaging and subtracted from the observed visibilities there will still be occasional large values where the RFI model fails to completely represent the more rapidly changing portion of the interference. As was demonstrated in Section V-A2, a subsequent clipping based on excessive residuals can suppress these outliers.

The data set from which the data in Figures 1 and 2 were extracted were imaged using two RFI suppression schemes. The first was to simply flag the channels in which strong RFI was observed and image the resulting data. The result of this is shown in Figure 6; the effects of the broadband interference are clearly seen. The second image, shown in Figure 7, was made from data from which an RFI model was subtracted, and subsequent outliers clipped (shown in the left plots of Figures 1 and 2). The image in Figure 7 has a much lower level of visible artifacts due to interference although some are still visible. These remaining artifacts are likely due to broadband interference which was inadequately modeled in the narrow band channels.

C. Example 3: Low Resolution RFI Excision/Flagging

The frequency resolution in the raw data was much higher than needed to avoid bandwidth smearing in the imaging and was designed to allow flagging of the narrow band signals with minimal loss of data. Imaging is generally done with a frequency resolution reduced by a factor of 10. An alternate

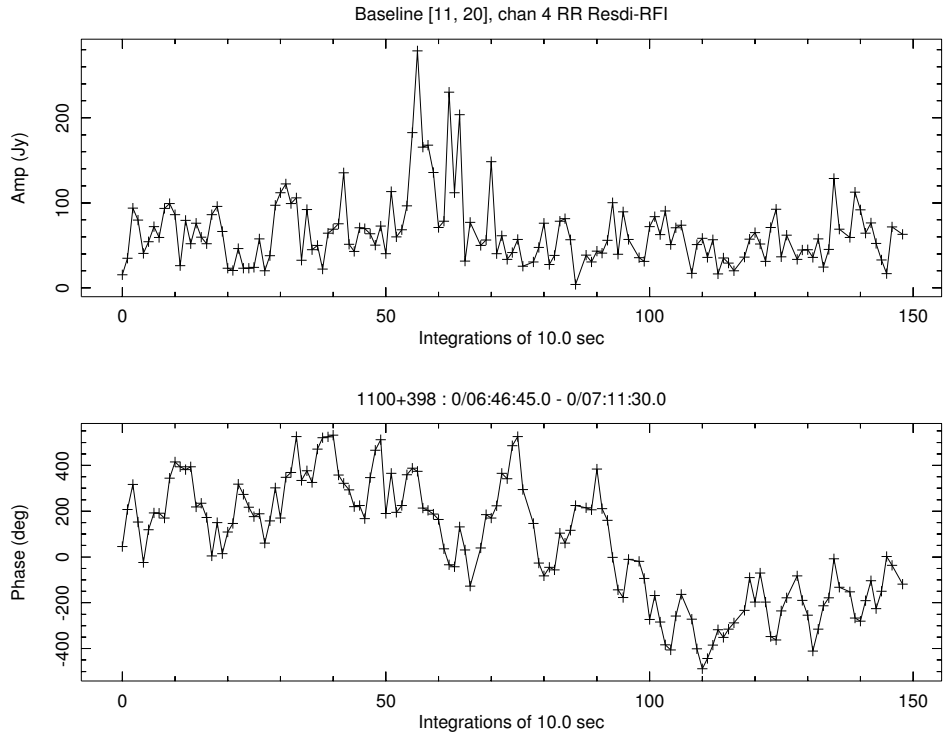

Fig. 5. Data in Figure 3 with the RFI model in Figure 4 subtracted.

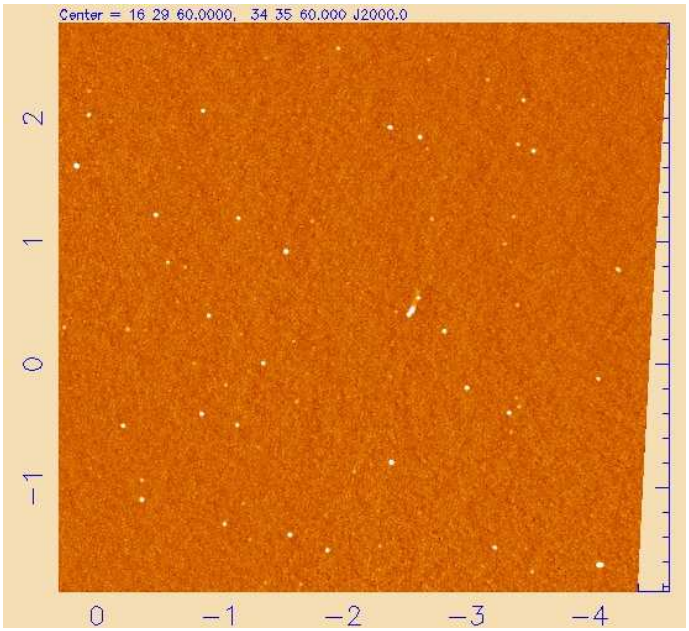

Fig. 8. Like Figure 6 but only removing interference from the low frequency resolution data. The RMS in the center portion of the image is 69.3 mJy. Image is the square root of a selected range of pixel values.

approach to RFI excision was applied to reduce the effects of broadband interference. The comb of strong narrow-band interfering signals prominent in Figure 2 were flagged and the data averaged from 127 to 12 channels, excluding the end channels. This data were then subjected to the following procedure:

1) **Initial imaging**
   The initial 12 channel data were imaged using IonImage without peeling of strong sources. At this stage, the residual interference in the data can degrade the self–cal solutions in the peeling to the point that serious artifacts are introduced around the bright source which then get incorporated in the RFI model and propagate through subsequent processing.
2) **RFI model calculation and subtraction**
   Obit task LowFRFI is used with timeAvg=1.0 (min) and minRFI=50 (Jy) to calculate the RFI model from the residual data from the previous imaging. This RFI model is subtracted from the initial data.
3) **Reimage with Peeling**
   The RFI subtracted data is then re-imaged using IonImage allowing Peeling if the field contains strong sources.
4) **Clipping residuals**
   A set of flags is derived from the residuals visibilities derived in the previous step. This uses Obit task AutoFlag with VClip=[100.,0.1], IClip=[100.,0.1] and RMSClip = [150.,0.1] These flags are written to an AIPS FG table on the RFI model subtracted data.
5) **Final imaging**
   IonImage is rerun as before but applying the flags derived in the previous step.

When this procedure was applied to the data described in Section V-B, the resulting final image is that represented in Figure 8. A comparison with the image shown in Figure 7 show that the visible RFI artifacts have largely been removed.

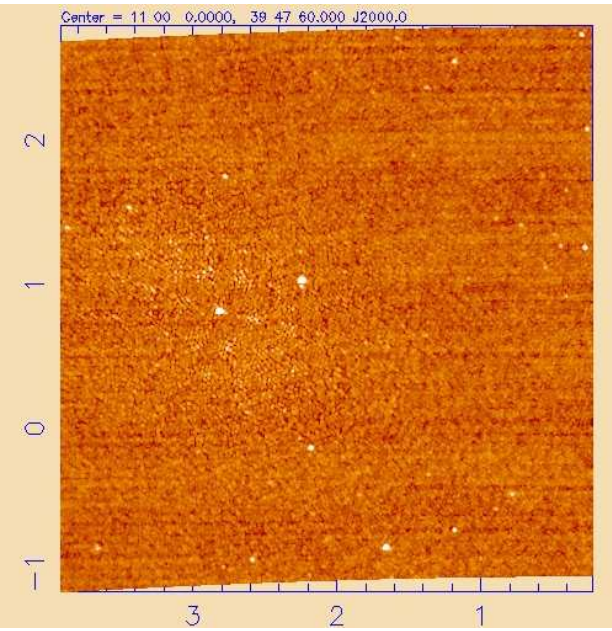

Fig. 9. Image of section of the 1100+398 field without removing interference. The interferences is visible in the horizontal banding. The scale in degrees is shown on the side of the image. The RMS in the center portion of the image is 96.4 mJy. Image is the square root of a selected range of pixel values.

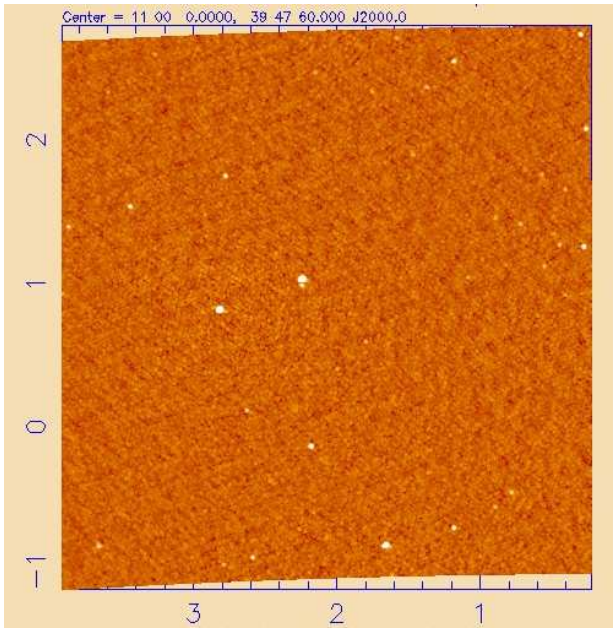

Fig. 10. Like Figure 9 but after RFI subtraction and clipping. The RMS in the center portion of the image is 79.9 mJy. Image is the square root of a selected range of pixel values.

TABLE I
COMPARISONS OF RFI SUPPRESSION OF SEVERAL VLSS FIELDS

Field	VLSS RMS mJy	Raw RMS mJy	RFI Sub mJy	RFI Sub + Clip mJy
0900+398	102.9	103.0	87.5	74.6
1100+398	101.5	96.5	81.3	79.9
1630+346	69.2	78.7	78.4	69.3

D. Examples 4: Further Low Resolution RFI Excision/Flagging

Image statistics are a useful metric for the effectiveness of RFI excision. In the following a number of VLSS pointings are analyzed following the scheme defined in Section V-C and the off-source RMS of the inner portions of the images at various stages compared in Table I. In this table, the column "VLSS RMS" gives the central pixel RMS from the VLSS survey processing images, "Raw RMS" is from the imaging with no RFI subtraction or peeling, "RFI Sub" is the RMS after RFI subtraction and "RFI Sub + Clip" is after a final clipping of residuals. The various fields are discussed below.

1) 0900+398: This field contains three sources brighter than 15 Jy which benefited from peeling. The phases for Antenna 25 were bad for the first 2 of 3 scans and data involving this antenna in those scans were flagged for the final image. Processing started with the final 12 channel averaged data from the VLSS pipeline.

2) 1100+398: Processing started with the final 12 channel averaged data from the VLSS pipeline. This field contained a single bright source that benefited from peeling. This data set was self calibrated in the VLSS processing which compromises the results far from the bright source. A section of the image without RFI subtraction or peeling is shown in Figure 9 and with RFI subtraction and peeling in Figure 10.

3) 1630+346: Processing of this data started from the 127 channel raw data and the VLSS calibration tables. This field contained a single bright source that benefited from peeling. This is data used in Examples 1 and 2, the final image is shown in Figure 8. While the image statistics for the final image and that from the VLSS survey are similar, the latter has a higher level of visible artifacts.

VI. DISCUSSION

The previous sections have demonstrated the efficacy of a technique for estimating and subtracting the contribution of earth based interfering signals from radio interferometer data. This technique is based loosely on that of Athreya[1]. The general technique is to first image the data, applying traditional flagging based RFI removal as needed to derive an initial sky model. This sky model is then subtracted from the observed data to derive a set of residual data which, in the limit of perfect imaging, will consist of noise plus the interfering signal. This residual data set is then counter rotated by the interferometer model which has the benefit of making terrestrial signals have constant phase and any residual celestial signals will have a phase that rotates with time. Averaging of this counter–rotated data will tend to wash out the residual celestial signal, beat down the noise while leaving a constant terrestrial signal unchanged. A final RFI model is then derived from this averaged, counter–rotated residual data using several criteria intended to determine when this data is dominated by interference. The RFI model is then interpolated and subtracted from the observed data.

In practice, the interfering signal is not constant over the averaging interval. In cases of strong impulsive interference

this may badly distort the RFI model in which case an initial flagging of these data may be beneficial. Less serious variation in the interference may leave significant residuals in the corrected data. These cases can be identified and flagged based on the residuals from the imaging of the RFI corrected data.

The residual based RFI subtraction scheme described above is useful for removing strong, quasi–constant narrow-band signals from high resolution data, it works less well on broad-band interfering signals when applied to high resolution data. Since the imaging requirements on the frequency resolution needed to avoid bandwidth smearing are less than that for RFI removal, the data are usually averaged by a factor of 10 before imaging. The RFI subtraction technique can be applied twice, once to the high resolution data to remove the very strong (up to 10s of thousands of Jy) and then a second time after averaging in frequency to remove the broadband interference (up to $\sim$1000 Jy in the data studied here).

Several potential problems have been identified in this study. The first of these is that use of peeling in generating the RFI model may lead to artifacts around the peeled sources that are not removed at later stages of processing. This is due to the degraded performance of self–calibration in the presence of interference; this leads to poor solutions and artifacts in the sky model used to form the residual data. These artifacts can then be incorporated in the RFI model and will not be removed later.

The second potential problem is that the process allows, in the limit of timeAvg=timeInt and minRFI=0, the residual data being subtracted unmodified from the observed data giving essentially the sky model visibilities without noise. This can be used to reduce the "noise" in the images produced to an arbitrary level. Care must be exercised not to simply throw enough parameters at the problem to obtain a desired "noise".

VII. Conclusions

A combination of traditional RFI flagging and a technique to estimate and subtract interfering signals is shown to be beneficial. An implementation is available in the Obit package. While the technique described above has only been applied to VLA 74 MHz data, it should be applicable to other cases of quasi-continuous interference.

Acknowledgment

The author thanks Huib Intema of NRAO, Joe Helmboldt of NRL and Ramana Athreya of the National Centre for Radio Astrophysics, Pune, India, for stimulating discussions.

References

[1] R. Athreya, "A New Approach to Mitigation of Radio Frequency Interference in Interferometric Data," *ApJ*, vol. 696, pp. 885–890, May 2009.
[2] W. D. Cotton, "Obit: A Development Environment for Astronomical Algorithms," *PASP*, vol. 120, pp. 439–448, 2008.
[3] Thompson, A. R. and Moran, J. M. and Swenson, Jr. G. W., *Interferometry and Synthesis in Radio Astronomy, 2nd Edition*, J. M. M. A. R. Thompson and G. W. Swenson, Eds. A Wiley-Interscience publication, Apr. 2001.
[4] A. S. Cohen, W. M. Lane, W. D. Cotton, N. E. Kassim, T. J. W. Lazio, R. A. Perley, J. J. Condon, and W. C. Erickson, "The VLA Low-Frequency Sky Survey," *Astron. J.*, vol. 134, pp. 1245–1262, Sep. 2007.
[5] W. D. Cotton, "Ionospheric Effects and Imaging and Calibration of VLA Data," *EVLA Memo Series*, vol. 118, pp. 1–12, 2007.